Out-Diffusion and Precipitation of Copper in Silicon: An Electrostatic Model

Christoph Flink,* Henning Feick, Scott A. McHugo,† Winfried Seifert, Henry Hieslmair, Thomas Heiser,‡ Andrei A. Istratov, and Eicke R. Weber

Department of Materials Science, University of California at Berkeley and Lawrence Berkeley National Laboratory, Berkeley, California 94720

(Received 4 August 1999)

Concentrations of mobile interstitial copper and precipitated copper in silicon were studied after a high temperature intentional contamination and quench to room temperature. It was found that below a critical contamination the copper predominantly diffuses out to the surface, while for higher initial copper concentrations it mainly precipitates in the bulk. The critical copper contamination equals the acceptor concentration plus 10^{16} cm^{-3}. This behavior can be explained by the electrostatic interaction between the positively charged interstitial copper and the forming copper precipitates.

PACS numbers: 61.72.Ss, 61.72.Cc

The introduction of copper interconnects in silicon integrated circuit technology has drastically increased the danger of unintentional in-diffusion of copper into silicon substrates. Consequently, the understanding of the physical behavior of copper in silicon and its reaction paths has become an important issue in semiconductor materials science and device technology. Among all transition metals, copper has the highest solubility in the silicon lattice at elevated temperature [1,2]. While at room temperature the equilibrium concentration of interstitial copper drops to a negligible level, it remains highly mobile [3]. Interstitial copper is a single donor with a level close to or even in the conduction band, compensating shallow acceptors [1]. Copper-acceptor pairing can significantly reduce the effective diffusivity of copper in p-type silicon [3,4]. However, this interaction is too weak for effective trapping of copper at room temperature [5]. Only a small fraction of the in-diffused copper forms stable point defects and complexes with mixed covalent-ionic character [6–8]. In fact, most of the supersaturated interstitial copper follows one of two distinct reaction paths discussed in literature: out-diffusion to the surface and precipitation in the bulk. Transmission electron microscopy (TEM) studies suggested that after introduction of 10^{17}–10^{18} cm^{-3} copper, most of the copper precipitates in the bulk upon cooling [9–11]. In n-type silicon it was found that with cooling rates larger than 100 K s^{-1} the precipitates form platelike defects throughout the bulk of presumably Cu_3Si, mainly on $\{111\}$ habit planes. These defects introduce bandlike states in the upper half of the band gap, as has been studied with deep level transient spectroscopy (DLTS) [10–13]. Copper precipitates are electrically amphoteric, i.e., they display a change in their charge state from positive to negative as the Fermi level is raised above the neutrality level at about E_C-0.2 eV [10,13]. In contrast to silicon contaminated with very high copper concentrations, total x-ray fluorescence (TXRF) studies on p-type silicon with copper contamination levels around 10^{14}–10^{15} cm^{-3} demonstrated complete out-diffusion of copper to the surface after both slow cool [14] and quench [15]. The objective of this Letter is to determine the conditions under which copper diffuses out to the surface or precipitates in the bulk, and to understand why it chooses the one or the other reaction path.

We have investigated p-type dislocation-free floating zone (FZ) and Czochralski (Cz) grown silicon with doping concentrations in the range of 10^{14} to 10^{16} boron atoms per cm^3 after high temperature copper in-diffusion of 10^{13} to 10^{17} cm^{-3} and quench. Interstitial copper concentrations have been measured with the transient ion drift (TID) technique [16,17]. The concentrations of precipitated copper in the bulk were measured by synchrotron-based x-ray fluorescence (XRF) at beam line 10.3.1 at the Advanced Light Source [18]. Details in the sample preparation can be found in Refs. [16–19].

Although interstitial copper is unstable in the silicon lattice at room temperature, significant amounts of copper remain dissolved for some hours after quenching the samples in silicon oil, ethylene glycol, or 10% NaOH, with quenching rates between 500 and 2000 K s^{-1}. Cooling the samples in air, however, which corresponds to a quenching rate of approximately 100 K s^{-1}, is not sufficiently fast to keep the copper in the interstitial state. Furthermore, neither the TID measurements nor the XRF results differed for the three fast quenching liquids. Likewise, no differences could be observed by comparing FZ and Cz grown silicon. For this reason we do not specify the quenching rate nor the growth method throughout this Letter.

In Fig. 1 we show the interstitial copper concentration as measured with TID 30 min after quench vs the solubility of copper at the in-diffusion temperature as given in Ref. [2]. For each of the three differently doped samples, a lower and a higher copper contamination region can clearly be recognized. At a relatively low copper contamination, the concentration of interstitial copper increases monotonically with the solubility concentration until it reaches a maximum at a certain critical contamination level. Beyond this critical contamination level the observed interstitial copper concentration decreases with increasing solubility. The critical copper contamination level has

 0031-9007/00/85(23)/4900(4)$15.00 © 2000 The American Physical Society

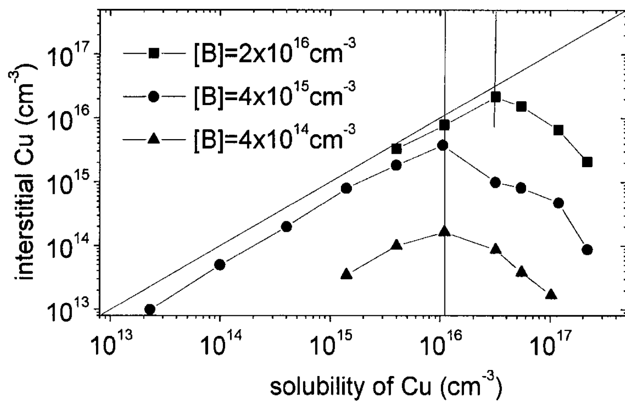

FIG. 1. Interstitial copper concentration as measured with TID 30 min after quench at room temperature vs the solubility concentration of copper at in-diffusion temperature.

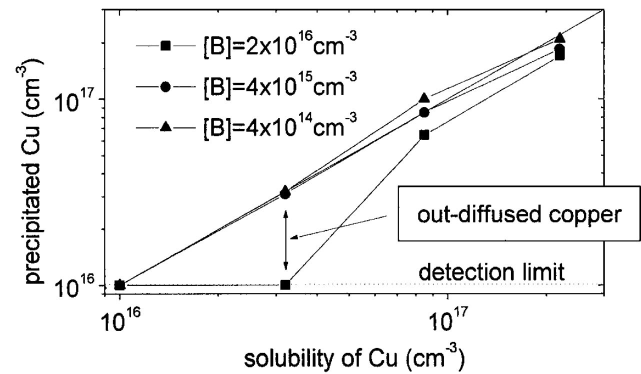

FIG. 2. Copper concentration measured with XRF vs the solubility concentration of copper at the in-diffusion temperature.

been found to depend on the doping concentration. While its value approximately matches for the two lower doped samples, the critical concentration for the sample doped with 2×10^{16} cm^{-3} is significantly shifted to a higher value. As a rule of thumb, the value of the critical copper contamination level equals the acceptor concentration plus 10^{16} cm^{-3}.

In order to determine the main reaction path of the copper above the critical contamination level, we show in Fig. 2 the bulk concentration of precipitated copper as measured with XRF vs the solubility of copper at the in-diffusion temperature for the same three doping concentrations as in Fig. 1. These measurements were performed after sufficient storage time at room temperature allowing the interstitial copper to complete its preferred reaction path, i.e., to diffuse out to the surface or to precipitate in the bulk. It can be seen that for all samples with an initial copper concentration larger than the critical contamination level, as defined in Fig. 1, the concentration of precipitated copper approximately equals the copper solubility. Thus, if the copper contamination exceeds the critical level, bulk precipitation is the main reaction path of the interstitial copper. Furthermore, the study of bevel-polished samples with the XRF microprobe did not detect a profile of precipitated copper. Hence, in the case of precipitation, most of the copper precipitates immediately after or during quench, i.e., significantly faster than out-diffusion could occur.

On the contrary, if the copper contamination is below the critical concentration, out-diffusion is the predominant mechanism. This can be seen in Fig. 2, where no precipitated copper was detected for the sample doped with 2×10^{16} boron atoms per cm^3 after in-diffusion of copper to an amount that equals the critical copper contamination level of 3×10^{16} cm^{-3} for this particular sample. Since XRF detects all copper regardless of its state, precipitated or dissolved, the missing copper has diffused out of the bulk. Because of the detection limit of 10^{16} copper atoms per cm^3, lower contamination levels could not be accessed by XRF.

To further elucidate the reaction path of the copper at subcritical contamination, we studied the interstitial copper concentration as measured with TID vs storage time at room temperature. In Fig. 3 results for three samples with an identical boron doping concentration of 6×10^{15} cm^{-3} and with an identical initial copper contamination of 5×10^{15} cm^{-3} but with varying thickness of 325, 650, and 990 μm are shown. Under these conditions the maximum concentration of copper measured with TID after quench can be close to the solubility concentration of copper at the in-diffusion temperature, while the concentration of interstitial copper decreases with time. The decay is nonexponential and slows down during storage at room temperature. Furthermore, the rate of the decay decreases with increasing sample thickness. Such dependence can be understood by an out-diffusion process. While a bulk precipitation rate would not depend on the thickness of the sample, an out-diffusion rate decreases with the distance the copper ions have to migrate to the surface, i.e., with the sample thickness. The out-diffusion of interstitial copper in p-type silicon can be simulated using a copper-dependent effective diffusivity adapted from Reiss *et al.* [14]. In the case of $N_{\mathrm{Cu}} \leq N_A$ the effective diffusivity D_{eff} is given by

$$D_{\mathrm{eff}}[N_{\mathrm{Cu}}(z)] = D_{\mathrm{int}} \times \left[1 + \frac{\frac{1}{2}[N_{\mathrm{Cu}}(z) - N_A + \frac{1}{\Omega}]}{\sqrt{[N_{\mathrm{Cu}}(z) - N_A - \frac{1}{\Omega}]^2 + \frac{N_{\mathrm{Cu}}(z)}{\Omega}}} \right],$$

where $N_{\mathrm{Cu}}(z)$ is the mobile interstitial copper concentration at the wafer depth z and N_A is the acceptor concentration. The intrinsic diffusivity of interstitial copper at room temperature equals $D_{\mathrm{int}} = 2.7 \times 10^{-7}$ cm^2/s and the pairing constant of copper-boron at room temperature and for $N_A \leq 10^{17}$ cm^{-3} is $\Omega = 1.6 \times 10^{-15}$ cm^3; both

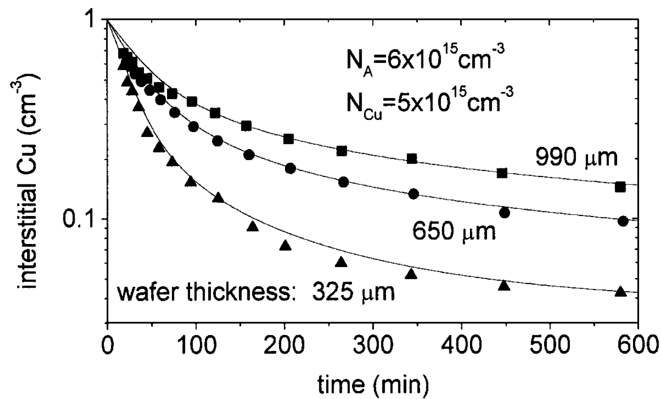

FIG. 3. Interstitial copper concentration vs storage time at room temperature after quench. Symbols represent measurement points as achieved with TID. Lines are simulation results assuming out-diffusion kinetics and no precipitation.

values are calculated from formulas given in Ref. [3]. For $N_{\mathrm{Cu}} \ll N_A$ the effective diffusion coefficient becomes the copper concentration independent formular given in Ref. [3]. Moreover, if the copper concentration approaches the boron concentration, field-enhanced diffusion has to be taken into account. Because the TID technique measures the interstitial copper concentration in the space charge region of a reverse biased Schottky diode, we compare the TID measurement results with concentration taken at the first micrometers of simulated concentration profiles. The simulations assume out-diffusion kinetics based on Fick's law and no precipitation. Including boundary conditions that suppose a repulsive surface potential of approximately 50 to 100 meV could fit the data well, as shown in Fig. 3. The origin of such an additional effect could be that the existence of a surface band bending impacts the out-diffusion conditions of the positively charged copper ions. Introducing a surface segregation layer with a segregation coefficient defined by the surface potential can simulate these conditions [19]. Thus, the interstitial copper concentrations measured with TID can be well explained by the out-diffusion of the copper.

Next, it can be seen in Fig. 1 that the interstitial copper concentrations measured with TID 30 min after quench depend strongly on, and never exceed, the doping concentration. This observation can be understood by the effect of the copper concentration dependent effective diffusion coefficient and the boundary conditions on the slope of the out-diffusion profile, rather than by partial precipitation within the lower copper contamination region. Lower doping concentrations lead to faster out-diffusion and a larger concentration difference between the near surface region and the bulk of the wafer. Under certain conditions, the interstitial copper concentration can be orders of magnitude higher in the bulk than measured with TID in the near surface region. If the copper concentration exceeds the doping concentration conductivity-type inversion may occur, introducing an additional drift effect due to an internal junction. We infer that within the lower copper contamination region, out-diffusion of the interstitial copper to the sample surface is the predominant reaction path.

Within the higher copper contamination region, small amounts of interstitial copper are still observed with TID; see Fig. 1. This indicates that at some point, after large amounts of copper have precipitated, the precipitation process slows down drastically and the remaining interstitial copper diffuses out.

In the following, we show that all experimental observations can be explained consistently by a model based on the position of the Fermi level. In Fig. 4 the maximum interstitial copper concentration as measured with TID is plotted vs the Fermi level position at room temperature. Motivated by the fact that the critical contamination level was found to be independent of the three fast quenching rates, the Fermi level position was calculated from the concentration of acceptors and the initial copper donor concentration at the in-diffusion temperature. For an initial copper concentration lower than the acceptor concentration, the Fermi level is in the lower half of the band gap and rises slowly with increasing copper contamination. When the copper concentration exceeds the doping level, the conductivity type changes from p to n type. This is, however, not sufficient to change the precipitation behavior of copper. Only when the Fermi level exceeds a critical value of about E_C-0.2 eV, does precipitation take place. Remarkably, this critical Fermi level position at about E_C-0.2 eV corresponds to the neutrality level of the copper precipitates as observed in n-type silicon [10–13]. It should be noted that the precipitates found in p-type Si after quench are identical in morphology and reveal similar bandlike states in the upper half of the band gap, as has been shown with high-resolution transmission electron microscopy (HRTEM) and minority carrier transient spectroscopy (MCTS), respectively [19]. This enables us to put forward the model that the precipitation of copper is determined by the electrostatic interaction between the positively charged copper ions and the copper precipitates.

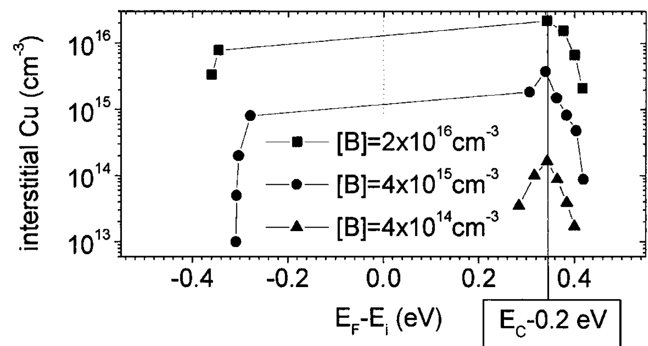

FIG. 4. Interstitial copper concentration as measured with TID 30 min after quench at room temperature vs the Fermi level position immediately after quench. The Fermi level was calculated from the acceptor concentration and the initial copper donor concentration at the in-diffusion temperature.

The precipitates are positively charged if the Fermi level is below their neutrality level and Coulomb repulsion will retard precipitation. If the Fermi level rises above the critical level of E_C-0.2 eV, the precipitates become neutral or negatively charged and precipitation can occur uninhibitedly. As the copper precipitates, the interstitial copper concentration decreases and the Fermi level drops below its critical value, resulting in positively charged precipitates, and the precipitation process slows down drastically.

These results imply that in p^+-type silicon copper always diffuses out, while the room temperature out-diffusion process in such highly doped silicon can take more than a year before being completed. This could result in long-term instabilities of copper contaminated devices on p^+-type silicon wafers.

In conclusion, we have shown that a simple electrostatic model can describe satisfactorily the observed difference in the out-diffusion and precipitation behavior of copper in silicon. To our best knowledge, this is the first precipitation process explained by an electrostatic model.

The authors are very grateful to G. Nimtz at the University of Cologne for his support. The authors are thankful to R. Falster from MEMC, to R. Knobel, W. Hensel, and D. Gilles from Wacker, and to F. G. Kirscht from Mitsubishi Silicon America for the silicon wafer supply. This work was supported by the Silicon-Wafer-Engineering-and-Defect-Science (Si-WEDS) consortium, which is supported by the National Science Foundation (NSF), and by the National Renewable Energy Laboratory (NREL), which is funded through the U.S. Department of Energy (DOE), under Contract No. XAF-8-17607-04. The use of experimental facilities at the Lawrence Berkeley National Laboratory (LBNL), in particular the use of the Advanced Light Source (ALS) and the National Center of Electron Microscopy (NCEM), is acknowledged. LBNL is funded through the Director, Office of Energy Research, Office of Basic Energy Sciences, Materials Sciences Division, of the DOE under Contract No. DE-AC03-76SF00098.

*Present address: Intel Corporation, RA2-275, 2501 NW 229th Street, Hillsboro, OR 97124.
Electronic address: Christoph.P.Flink@Intel.com

†At the Advanced Light Source (ALS) at the Lawrence Berkeley National Laboratory (LBNL), MS 2-400, 1 Cyclotron Road, Berkeley, CA 94720.

‡Now at the Laboratore de Physique et Application des Semiconducteurs, CNRS, Universite Louis Pasteur, BP 20, F–67037, Strasbourg Cedex 02, France.

[1] R. H. Hall and J. H. Racette, J. Appl. Phys. **35**, 379 (1964).
[2] E. R. Weber, Appl. Phys. A **30**, 1 (1983).
[3] A. A. Istratov, C. Flink, H. Hieslmair, E. R. Weber, and T. Heiser, Phys. Rev. Lett. **81**, 1243 (1998).
[4] H. Reiss, C. S. Fuller, and F. J. Morin, Bell Syst. Tech. J. **35**, 535 (1956).
[5] P. Wagner, H. Hage, H. Prigge, Th. Prescha, and J. Weber, in *Semiconductor Silicon 1990: Proceedings of the 6th International Symposium on Silicon Materials Science and Technology,* edited by H. R. Huff, K. G. Barraclough, and J.-I. Chikawa (Electrochemical Society, Pennington, NJ, 1990), p. 675.
[6] A. A. Istratov and E. R. Weber, Appl. Phys. A **66**, 123 (1998).
[7] T. Heiser, A. A. Istratov, C. Flink, and E. R. Weber, Mater. Sci. Eng. B **58**, 149 (1999).
[8] S. K. Estreicher, Phys. Rev. B (to be published).
[9] K. Graff, *Metal Impurities in Silicon-Device Fabrication* (Springer-Verlag, Berlin, 1995).
[10] M. Seibt, M. Griess, A. A. Istratov, H. Hedemann, A. Sattler, and W. Schroeter, Phys. Status Solidi A **166**, 171 (1998).
[11] M. Seibt, H. Hedemann, A. A. Istratov, F. Riedel, A. Sattler, and W. Schroeter, Phys. Status Solidi A **171**, 301 (1999).
[12] A. A. Istratov, H. Hedemann, M. Seibt, O. F. Vyvenko, W. Schroeter, T. Heiser, C. Flink, H. Hieslmair, and E. R. Weber, J. Electrochem. Soc. **145**, 3889 (1998).
[13] A. A. Istratov, O. F. Vyvenko, C. Flink, T. Heiser, H. Hieslmaier, and E. R. Weber, in *Defect and Impurity Engineered Semiconductors II,* edited by S. Ashok, J. Chevallier, K. Sumino, B. L. Sopori, and W. Goetz, MRS Symposia Proceedings (Materials Research Society, Warrendale, PA, 1998), p. 313.
[14] M. B. Shabani, T. Yoshimi, and H. Abe, J. Electrochem. Soc. **143**, 2025 (1996).
[15] C. McCarthy, M. Miyazaki, H. Horie, S. Okamoto, and H. Tsuya, in *Semiconductor Silicon 1998: Proceedings of the 8th International Symposium on Silicon Materials Science and Technology,* edited by H. R. Huff, H. Tsuya, and U. Goesele (The Electrochemical Society, Pennington, NJ, 1998), p. 629.
[16] T. Heiser and E. R. Weber, Phys. Rev. B **58**, 3893 (1998).
[17] T. Heiser, S. McHugo, H. Hieslmair, and E. R. Weber, Appl. Phys. Lett. **70**, 3576 (1997).
[18] S. A. McHugo, A. C. Thompson, and H. Padmore, in *Defect and Impurity Engineered Semiconductors II* (Ref. [13]), p. 589.
[19] C. Flink, Ph.D. thesis, Cologne, Germany, 2000.